AIAA 80-1167R

# Modeling Calculations for HMX Composite Propellants

M. W. Beckstead*
*Brigham Young University, Provo, Utah*
and
K. P. McCarty†
*Hercules, Inc., Magna, Utah*

**HMX (cyclotetramethyline tetranitramine) composite propellants burn at rates significantly lower than HMX monopropellant. To model the behavior of these propellants, a new model was developed within the framework of the Beckstead-Derr-Price (BDP) modeling approach. A time-averaging approach has been developed assuming that the propellant burns through alternate layers of binder and oxidizer at significantly different rates. The model has been compared in detail with experimental results from 17 HMX/HTPB propellants. Both the data and the model show that there is only a small dependence of rate on particle size. The model predicts that the rates of HMX/HTPB propellants will converge with increasing solids loadings, and that above ~85% solids there is very little change in rate for varying formulations. The interpretation of the data using the model indicates three predominant mechanisms leading to the peculiar characteristics of HMX propellants. First, the HMX binder diffusion flame is an energy poor flame that robs energy from the products that would otherwise result from the monopropellant flame. Second, there appears to be a significant ignition delay time associated with large particles that impedes the overall rate. Third, the binder rate appears to be very significant. The model indicates that changing the rate using conventional catalysis approaches would be very difficult, since the rate is more dependent on binder decomposition characteristics than on the oxidizer.**

## Introduction

A MODEL has been developed to describe the combustion characteristics of HMX composite propellants. The model is based on several key concepts. First, the oxidizer and binder have different surface temperatures. Second, the model can handle up to three different oxidizer sizes. Third, the overall burn rate is calculated from a time-averaged approach rather than the conventional space averaging used in models based on the Beckstead-Derr-Price (BDP) model[1,2] (e.g., Refs. 1-6). A key contribution in the time-averaging approach is use of an ignition delay time for the oxidizer. Finally, a generalized flame standoff distance has been developed based on a modified Burke-Schumann diffusion flame analysis.

The combustion characteristics of HMX composite propellants are very different from those of ammonium perchlorate (AP) composite propellants. First, HMX monopropellant burns at a higher rate with a much higher adiabatic flame temperature (3200 K compared to 1400 K) than AP monopropellant. Second, the adiabatic flame temperature of AP propellants is ~2500-3000 K depending on the AP concentration. In comparison, the adiabatic flame temperature of HMX propellants is ~1800 to 2200 K for the same loading densities. Finally, AP propellants typically burn at rates higher than the monopropellant rate with a very strong dependence on particle size and concentration. HMX propellants burn at rates 3-10 times lower than the monopropellant rate with little dependence on particle size or concentration. These general observations force one to the conclusion that the controlling mechanisms in HMX propellants are significantly different than in AP propellants.

The phenomenological interpretation of these observations is outlined in Fig. 1 and discussed in this paragraph. With fine HMX, diffusion distances can be expected to be very short (i.e., less than the monopropellant flame height). This results in the relatively cool HMX/HTPB primary flame dominating the combustion and suppressing the rate below that of the monopropellant. However, with coarse HMX, the primary flame should not be able to dominate because of the increased diffusional distances. One would expect the larger crystals to burn at a rate approximating that of the monopropellant, and the propellant rate would also be expected to be close to that of the monopropellant. Window bomb movies do not allow a definitive resolution of individual HMX particles burning on the propellant surface, but the authors' interpretation of window bomb movies[7,8] is that large particles do indeed burn at a rate very near that of the monopropellant. Coarse crystals appear to ignite very slowly but burn out very rapidly leaving depressions on the propellant surface. The relatively short burn time combined with the long ignition time results in an unstable, erratic burning at the propellant surface. Statistically, very few crystals burn at the same time, with the net result being a much reduced burning rate. Large crystals reside on the surface as the binder burns by and then ignite and disappear rapidly.

At the beginning of the study, several exploratory modifications were made to Cohen's HMX model[5] and the Hercules' BDP model.[6] These two computer models were modified to try to simulate the types of propellants desired. Varying degrees of success were achieved, but it was concluded that neither Cohen's HMX model nor the Hercules' BDP model could be modified sufficiently to achieve all of the desired objectives. Therefore, a more comprehensive modeling effort was undertaken. The new modeling approach has been based on the concept that binder and oxidizer particle sizes have different surface temperatures. This approach has been labeled the separate surface temperature (SST) approach.

Also, it was determined that the conventional surface-averaging approach was not realistic, either phenomenologically nor numerically. Therefore, a time-averaging approach was developed as a more consistent basis for the modeling. In

Presented as Paper 80-1167 at the AIAA/SAE/ASME 16th Joint Propulsion Conference, Hartford, Conn., June 30-July 2, 1980; submitted Sept. 11, 1980; revision received May 7, 1981. 

*Professor, Dept. of Chemical Engineering. Associate Fellow AIAA.

†Superintendent, Combustion and Explosives Group.

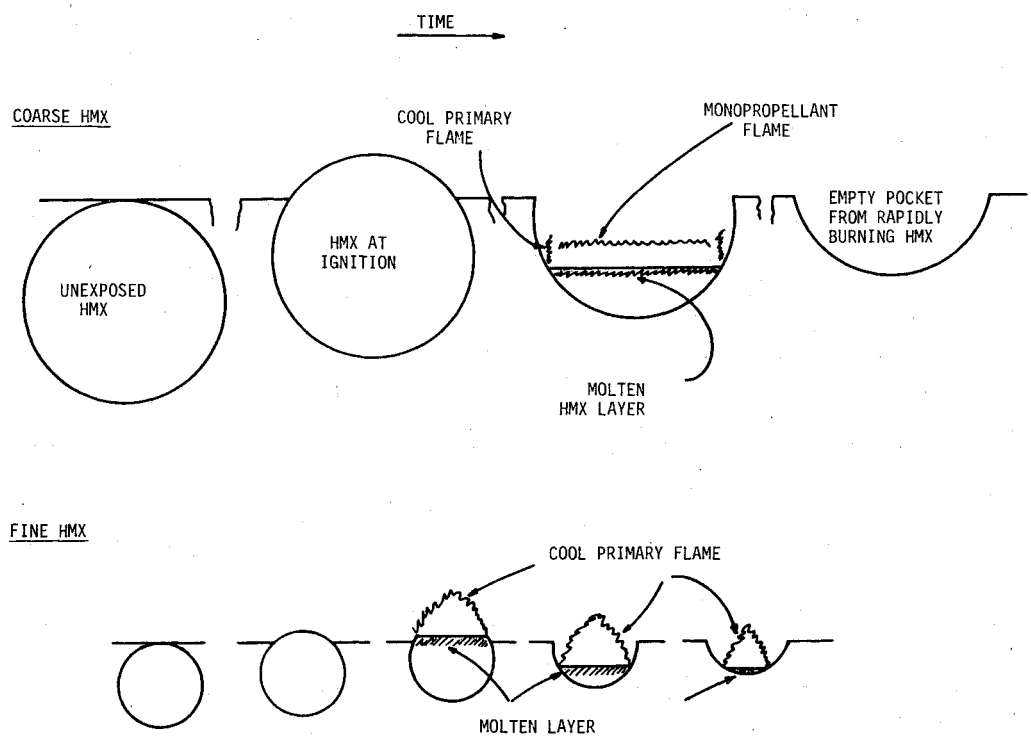


**Fig. 1 Phenomenological picture of HMX combustion evolution in composite propellants.**

addition, several other aspects of HMX propellant combustion have been considered and are discussed in the following paragraphs. The separate surface temperature approach is analogous to the two temperature model[9] developed in the late 1950's to describe ammonium nitrate composite propellants. All recent modeling efforts have considered the binder and oxidizer to have an averaged surface temperature.

The basic derivations of the overall separate surface temperature model have been presented previously[10,12,13] and will not be repeated here.

Another peculiar characteristic of HMX propellants is the change in pressure exponent that occurs typically somewhere between 7 and 21 MPa (1000 and 3000 psi).[5,7,8] The exponent break is apparently due to changes in the controlling combustion mechanism. The current study was performed for rocket motor applications, and the model was developed based on the mechanisms postulated to control the rate in that particular pressure regime. Little effort was directed at modeling the changes in mechanisms that lead to the exponent break.

## Inconsistencies of Surface Area Calculation

A serious discrepancy was discovered relative to the BDP approach of using oxidizer surface areas for application to HMX propellants. In the original BDP approach,[1,2] the burning surface area of the fuel and various oxidizer fractions were used throughout the model. The basic need for the surface areas comes from the space-averaged overall continuity equation

$$m_T S_0 = \sum_i m_{oxi} S_{oxi} + m_b S_b \qquad (1)$$

Where the summation occurs over each oxidizer size. Solving for the average linear burn rate yields

$$\bar{r} = \frac{1}{\rho_p} \sum_i m_{oxi} \frac{S_{oxi}}{S_0} + m_b \frac{S_b}{S_0} \qquad (2)$$

so that the surface areas are normalized with the total burn surface area.

In the original BDP model, the oxidizer surface area is assumed to be a spherical sector such as shown in Fig. 2. This is probably a reasonable assumption as long as the oxidizer and binder rates are similar and the protrusion or recession relative to the intersection plane is small. However, when the rates differ significantly or when the ignition delay time is too long, unrealistic surface areas result. Furthermore, for such limiting conditions the calculated surface area becomes large, reaching a maximum at the conditions shown in Fig. 2. This results in an abrupt discontinuity in the $S_{ox}$ calculations at the limiting conditions. AP propellants with very wide distribution, double-base propellants, and propellants containing HMX will all result in conditions where either the oxidizer binder rates are significantly different or where widely differing oxidizer distributions will lead to the unrealistic limiting conditions. Also, scanning electron microscope (SEM) examination of quenched samples shows crystals with relatively flat surfaces, although often with a rounded protrusion in the center. Therefore, an assumption of a planar oxidizer surface is more realistic than a spherical sector, considering the limiting conditions shown in the figure

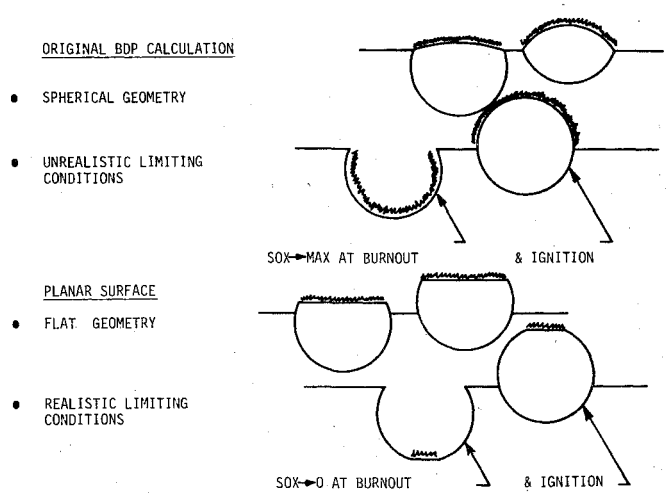


**Fig. 2 Comparison of surface area calculations for a spherical sector vs a flat surface.**

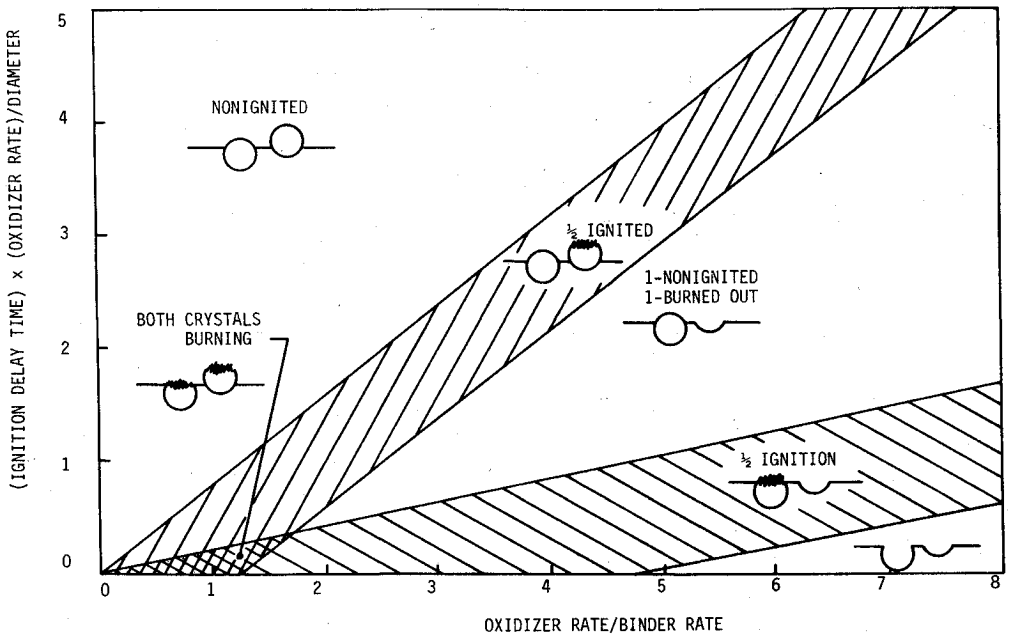


Fig. 3 Ignition delay time map.

or SEM photographs of quenched samples. Therefore, an equation for the oxidizer surface area was derived assuming a planar area.

Utilizing the planar area derivation, calculations were performed with the model that also proved to be numerically unstable. Although several approaches were attempted to eliminate the instabilities, none succeeded. The reason for the instability can best be visualized by examining a map of a normalized ignition delay time vs the ratio of oxidizer-to-binder rate as shown in Fig. 3. The shaded areas are the regimes where finite $S_{ox}$ values are calculated. It should be noted that the two shaded areas correspond to the two statistical oxidizer configurations discussed in the BDP model. In the nonshaded areas, $S_{ox}$ values of zero are calculated for the various configurations indicated. The upper shaded area corresponds to one-half of the oxidizer crystals burning and the other half not yet ignited. The lower shaded area corresponds to the other half of the crystals ignited with the first configuration burned out.

From this map, it is apparent that, for large ignition delay times or for oxidizer-to-binder rate ratios greater than ~2, both oxidizer configurations will not be burning simultaneously. Either one or the other or neither configuration could result. This is apparently what happens for HMX-composite propellants or AP propellants with very wide distributions where the rates of calculated binder and oxidizer vary significantly or where large ignition delay times result from low propellant burning rates. Figure 4 is a plot of burn rate vs surface temperature for AP, HMX, HTPB, and double base using typical activation energies and pyrolysis parameters for each ingredient. For the range of burn rates of interest the differences between HMX and HTPB are extremely dramatic. Their rates are totally different and one can expect an oxidizer to binder ratio of 5-10 being the norm.

The net result is that, statistically, few oxidizer crystals are burning on the surface at any one time. This can lead to a very unstable surface configuration, which leads to totally unrealistic results. It can also be shown that using the original BDP assumption of a spherical sector will lead to very similar unacceptable results. The fact that some computer versions of the BDP model do not show the instabilities is apparently due to assuming that the value of $S_{ox}$ calculated at the limiting condition persists indefinitely in time. This is obviously incorrect. Use of petite ensemble model (PEM)[3,4] statistics will tend to smear out the discontinuities, but for large ignition delay times and/or large discrepancies in the oxidizer-binder burning rates, even the PEM statistics will not fully resolve

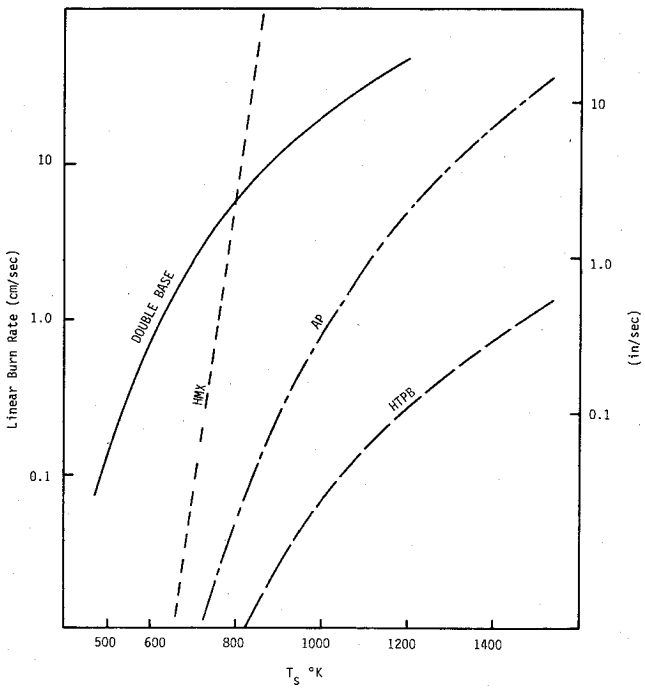


Fig. 4 Decomposition rates of common propellant ingredients.

the numerical problems caused by having empty and/or unignited status. Therefore, the conclusion ultimately was reached that the space-averaging BDP approach (i.e., any $S_{ox}$ calculation), if used consistently, will result in numerical instabilities and unrealistic physical limiting conditions.

## Time-Averaged Approach

### Time-Averaged Basis

The nature of the phenomenological picture that has evolved suggests that time averaging is required to give consistent results. The approach of assuming a time-averaged propellant surface is realistic on a physical basis because the binder and oxidizer appear to burn in series, rather than in parallel (as in the original space-averaged BDP concept). Strahle[14] has also recently proposed a time-averaging approach for modeling composite propellants. The equation for

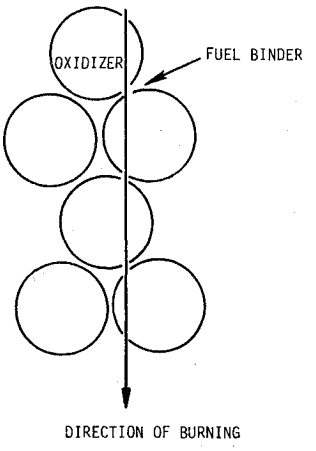


**Fig. 5 Time-averaged propellant burning.**

the average propellant burn rate is of the form

$$\bar{r}=\frac{\Sigma \text{ distances}}{\Sigma \text{ times}}=\frac{\Sigma \text{ distances}}{\Sigma \text{ (distances/rates + delay times)}} \tag{3}$$

The distances involved are an oxidizer dimension and an associated binder dimension. Figure 5 shows what occurs on a statistical basis. Burning will be somewhat random. However, for a sufficiently large sample it can be assumed that burning occurs approximately in a straight line through a packed bed of oxidizer/binder. The statistical intersection diameter for straight-line combustion is $D'=\sqrt{2/3}\,D_0$ (Refs. 15, 16). The intercrystal thickness of binder associated with a crystal is denoted as $\Delta_i$. It is calculated assuming that the binder is distributed according to the specific surface area of the individual particle sizes and that all of the binder forms an annulus around each particle.[12,13] Assuming that both oxidizer and binder burn at constant rates, the overall rate becomes

$$\bar{r}=\frac{\sum_i N_i(D_i'+2\Delta_i)}{\sum_i N_i\left(\frac{D_i'}{r_{oxi}}+t_{igni}+\frac{2\Delta_i}{r_b}+t_{bi}\right)} \tag{4}$$

where

$N_i$ = number of $i$th oxidizer crystals per unit volume
$D_i'$ = statistical intersection diameter of $i$th oxidizer size
$\Delta_i$ = distance from oxidizer edge to edge of assumed binder annulus
$t_{igni}$ = ignition delay time of $i$th oxidizer size
$t_{bi}$ = binder burnthrough time of $i$th oxidizer size
$r_{oxi}$ = rate of $i$th oxidizer
$r_b$ = average binder burn rate

The number of oxidizer crystals per unit volume of propellant can be calculated from the volume fraction as

$$N_i=\frac{\zeta_i}{(\pi/6)D_i^3} \tag{5}$$

where $\zeta_i$ is the volume fraction of the $i$th oxidizer size. Dividing Eq. (4) through by $D_i'$ yields a more convenient format

$$\bar{r}=\frac{\Sigma N_i D_i'(1+\delta_i)}{\sum_i N_i D_i'\left(\frac{1}{r_{oxi}}+\frac{t_{igni}}{D_i'}+\frac{\delta_i}{r_b}+\frac{t_{bi}}{D_i'}\right)} \tag{6}$$

where $\delta_i=2\Delta_i/D'$. For a monomodal HMX propellant, where $r_{ox}\gg r_b$, the first term in the denominator is small, and the propellant rate approaches the binder rate multiplied by some factor which is dependent on the ignition delay time and increases with increased solids loading,

$$\bar{r}_{mono}=r_b\left(\frac{1+\delta}{\delta+\frac{t_{ign}r_b}{D'}+\frac{t_b r_b}{D'}}\right) \tag{7}$$

This expression will give qualitative agreement with experimental data for HMX propellants only if the second term in the denominator is large compared to the other terms. Also, to have the rate decrease with increasing particle size as observed experimentally, the ignition delay time must be proportional to the diameter to a power greater than one. For large ignition delay times and low binder rates the form of the time-averaged equation will give the proper trends.

Incomplete reaction of the binder affects the burn rate, especially in HMX composite propellants. Windowbomb movies[7,8] show shedding of layers of binder from the burning surface of HMX composite propellants. Stoichiometry indicates that HMX composite propellants burn very fuel rich. It is probable that all of the fuel is only partially oxidized or, more likely, that part of the fuel does not even react. The windowbomb movies seem to indicate the latter is more accurate; that sheets of binder lift from the surface unreacted.

To simulate the effect of unreacted binder within the model, two terms were introduced into the model. The first was a fraction binder reacted ($fr_b$) term which was incorporated into the surface energy balances for binder and oxidizer and must be incorporated into the time-averaged equation. The second, the binder burnthrough time ($t_b$), is incorporated into the time-averaged equation above. The final equation for the time-averaged rate is

$$\bar{r}=\frac{\sum_i N_i D_i(1+\delta_i)}{\sum_i N_i D_i\left[\frac{1}{r_{oxi}}+\frac{t_{igni}}{D_i'}+\frac{\delta_i fr_{bi}}{r_b}+\frac{t_{bi}(1-fr_{bi})}{D_i'}\right]} \tag{8}$$

This time-averaged burn rate equation has been programmed in the computer model. The summation occurs over both oxidizer size and type, allowing two types of oxidizer and three sizes of oxidizer.

#### Fraction of Binder Reacting

Quantitative data are not available to allow estimation of the fraction of binder that does react as a function of pertinent variables. Based on the windowbomb movies,[7,8] binder shedding appeared to be much worse at low pressures than at high but did not appear too dependent on particle size or solids loading. Logically, it would seem that the amount of binder reacting should depend principally on the energy feedback from the primary flame over the binder. It would appear to be related to the initial temperature and possibly the stoichiometry. Therefore, the following function was assumed

$$fr_{bi}=f_a fr_{bpFi}\left(\frac{T_0}{298}\right)e^{-\xi_{PFi}} \tag{9}$$

where $f_a$ is an arbitrary constant. By matching the data with the $f_a$ as an arbitrary constant it was found to require a value of $\sim 1.2$. The assumed form seems reasonable and appears to give the appropriate dependencies. However, this is an area that warrants further thought, analysis, and experimental data.

#### Binder Burnthrough Time

Simultaneously with the development of the current work, Strahle[14] proposed a format for the binder burnthrough concept. The binder burnthrough time is meant to represent

the unsteady nature of binder pyrolysis in a propellant environment, particularly in fuel-rich situations. As an oxidizer burns, the binder adjacent to the oxidizer is heated by the primary flame, with the resultant pyrolysis products participating in the flame. However, as the oxidizer burns out, particularly in cases where the oxidizer rate is much faster than the binder rate, there is no direct heat source to continue heating the binder, except the energy stored in the thermal wave. At this point, the pyrolysis will slow down and possibly stop. For the remaining binder to burn or sluff off, energy must be robbed from an adjacent particle. Alternatively, if an underlying particle gets ignited from another direction, it could burn under the binder, resulting in the binder sluffing off. This effect has been seen in the windowbomb movies. Strahle considered two- and three-column models to simulate these effects. Within the current model, only the form of Strahle's burnthrough time has been used. The equation for the burnthrough time is

$$t_b = f_d \Delta_i \exp(\Delta_i r_b/\alpha_t)/\bar{r} \tag{10}$$

where $\alpha_t$ is the thermal diffusivity and $f_d$ is a proportionality constant. Thus, the burnthrough time increases with increasing interparticle distance and decreases with increasing average rate. The exponential term approaches unity for most cases that have been considered. The equation for the burnthrough time has been incorporated into the computer program and used in conjunction with the time-averaged rate equation.

#### Ignition Delay Time

The postulated ignition delay time results from the discontinuous nature of composite propellants (i.e., the crystals are not necessarily in good thermal contact with the binder). The ignition delay time is the time it takes an oxidizer crystal to ignite, assuming that the ignition process starts when a crystal first becomes exposed to the burning surface. As the burning surface sweeps over the crystal, heat is fed to the crystal, which heats up and starts to decompose. The time required for this process to occur is the ignition delay time.

The first attempt to incorporate this concept into a combustion model was made by Hermance[16] using data generated by Shannon[17] for weakly pressed AP strands. The BDP model and other derivative models have all incorporated the same idea and form of equation, which is

$$t_{ign} = C_{ign} D_0^{1.8}/P^{0.721} \tag{11}$$

In most of these models, varying the ignition delay time parameters has little effect on the net burning rate. However, as the current modeling progressed with HMX propellants, it soon became apparent that the ignition delay of the HMX crystals should be a dominant mechanism in determining the burn rate of the propellant. Furthermore, the previously used equation for ignition delay was developed for AP, and there are no corresponding data for HMX (pressed strands of HMX burn with a relatively thick molten layer on the surface). Therefore, a fundamental approach was undertaken to calculate the ignition delay time of a crystal in a propellant.

To incorporate a diameter dependence, a transient two-dimensional heat transfer analysis was set up, and a solution to the two-dimensional differential heat conduction equation was obtained from Carslaw and Jaeger.[18] However, it was concluded that the Carslaw and Jaeger solution cannot be applied directly because of nonuniform boundary conditions (i.e., heating occurs on only one side of the crystal). Rather than pursue this approach further, it was decided to use an empirical data correlation for the ignition delay time. From the derivation and from the data,[17] it is apparent that an ignition delay time should be proportional to the diameter raised to a power and inversely proportional to the rate.

$$t_{ign} = c_{ign} \frac{D_0^{(\delta_{ign})}}{r} \tag{12}$$

A linear regression analysis of Shannon's data for AP gives

$$t_{ign} = 4.321 \frac{\text{s}}{\text{cm}^{0.7}} \frac{D_0^{1.7}}{\bar{r}} \tag{13}$$

The similarity between Eqs. (11) and (13) is readily apparent. The difference is that use of burn rate in place of pressure as a variable is more accurate considering the transient heat-transfer equations. Use of burn rate also permits application of the equation to a non-AP oxidizer. Therefore, Eq. (12) is proposed as a more accurate replacement for Eq. (11) from the original BDP and Hermance models. Equation (12) has been programmed into the computer program and is being used for both HMX and AP calculations.

The ignition delay time should also be proportional to the chemical activity of the oxidizer. In other words, the higher the activation energy of the initial decomposition reaction, the longer the ignition delay time. After the crystal has been heated, there is probably a chemical induction time before ignition is established completely. Therefore, the ignition delay time should be proportional to the chemical activity in some form or another and to the ignition temperature. To simulate these effects, $c_{ign}$ was defined as

$$c_{ign} = \frac{E_s(T_{melt} - T_0)}{E_{ref}(T_{ref} - T_0)} \tag{14}$$

where $E_s$ is the surface reaction activation energy, $T_{melt}$ the melting temperature, and $E_{ref}$ and $T_{ref}$ arbitrary reference values. Obviously, additional work is needed in this area to refine the input to the model.

## HMX Propellant Calculations

#### Experimental Data

Calculations were performed for 17 HMX/HTPB propellants utilizing the model as just outlined. HTPB propellant tests giving burn rate data between 2.8 and 12.4 MPa (400 and 1800 psi) have been selected as the basic data bank.[7,8] To make a consistent comparison with the model, random fluctuations in the strand data had to be eliminated. Some of the strand data has excessive scatter; therefore, a data-smoothing procedure was used to eliminate the random scatter and obviously outlying points. This gives a total of 51 datum points providing variations of pressure, particle size, and concentration. This extensive data bank provides a very comprehensive comparison and verification for the model.

#### Predicted Rates and Exponents

The calculations tabulated in Table 1 include the pressure, the predicted rate, the experimental rate, the difference between predicted and experimental rates, and the propellant formulation. The overall results show the maximum deviation is $-22\%$. Greater than 95% of the predictions are within $\pm 20\%$, and $\sim 75\%$ are within $\pm 10\%$. Considering the extremely broad variation in formulations, the agreement is excellent.

To give a more graphic comparison of the results, the predicted values for 6.9 MPa (1000 psi) are plotted vs the experimental data in Fig. 6. All but three cases fall within $\pm 10\%$. The model is able to predict the correct burn rate and trends over a broad range of rates and formulations. The low point is a 78% solid, trimodal propellant. Figure 7 shows the predicted burn rate exponent plotted vs the experimental values. Considering the inherent scatter in obtaining the slope of burn rate data, the agreement between the predicted and experimental values is very good.

**Table 1 Comparison of experimental rates—HMX/HTPB propellants**

| Pressure | Predicted Rate cm/sec | Predicted Rate (in./sec) | Experimental Rate cm/sec | Experimental Rate (in./sec) | % Error | % HMX 400μ | % HMX 200μ | % HMX 58μ | % HMX 4μ |
|---|---|---|---|---|---|---|---|---|---|
| 1 | 0.119 | (0.047) | 0.122 | (0.048) | -1.2 | -- | -- | 70.00 | -- |
| 2 | 0.163 | (0.064) | 0.168 | (0.066) | -3.5 | -- | -- | 70.00 | -- |
| 3 | 0.203 | (0.080) | 0.224 | (0.088) | -9.1 | -- | -- | 70.00 | -- |
| 1 | 0.071 | (0.028) | 0.051 | (0.020) | -7.5 | 70.00 | -- | -- | -- |
| 2 | 0.107 | (0.042) | 0.104 | (0.041) | 1.6 | 70.00 | -- | -- | -- |
| 3 | 0.157 | (0.062) | 0.170 | (0.067) | -7.8 | 70.00 | -- | -- | -- |
| 1 | 0.191 | (0.075) | 0.178 | (0.070) | 7.8 | -- | -- | 35.00 | 35.00 |
| 2 | 0.264 | (0.104) | 0.241 | (0.095) | 9.6 | -- | -- | 35.00 | 35.00 |
| 3 | 0.356 | (0.140) | 0.318 | (0.125) | 12.1 | -- | -- | 35.00 | 35.00 |
| 1 | 0.120 | (0.047) | 0.107 | (0.042) | 12.0 | 35.00 | -- | 35.00 | -- |
| 2 | 0.150 | (0.059) | 0.145 | (0.057) | 3.4 | 35.00 | -- | 35.00 | -- |
| 3 | 0.211 | (0.083) | 0.196 | (0.077) | 8.4 | 35.00 | -- | 35.00 | -- |
| 1 | 0.178 | (0.070) | 0.152 | (0.060) | 16.2 | -- | 23.30 | 23.30 | 23.30 |
| 2 | 0.244 | (0.096) | 0.211 | (0.083) | 16.0 | -- | 23.30 | 23.30 | 23.30 |
| 3 | 0.330 | (0.130) | 0.287 | (0.113) | 14.7 | -- | 23.30 | 23.30 | 23.30 |
| 1 | 0.234 | (0.092) | 0.236 | (0.093) | -0.7 | -- | -- | -- | 78.00 |
| 2 | 0.320 | (0.126) | 0.325 | (0.128) | -1.2 | -- | -- | -- | 78.00 |
| 3 | 0.424 | (0.167) | 0.439 | (0.173) | -3.2 | -- | -- | -- | 78.00 |
| 1 | 0.178 | (0.070) | 0.188 | (0.074) | -6.1 | -- | -- | 78.00 | -- |
| 2 | 0.224 | (0.088) | 0.236 | (0.093) | -5.3 | -- | -- | 78.00 | -- |
| 3 | 0.257 | (0.101) | 0.295 | (0.116) | -12.8 | -- | -- | 78.00 | -- |
| 1 | 0.147 | (0.058) | 0.132 | (0.052) | 11.1 | -- | 78.00 | -- | -- |
| 2 | 0.188 | (0.074) | 0.185 | (0.073) | 1.2 | -- | 78.00 | -- | -- |
| 3 | 0.277 | (0.109) | 0.251 | (0.099) | 10.5 | -- | 78.00 | -- | -- |
| 1 | 0.130 | (0.051) | 0.137 | (0.054) | -5.1 | 78.00 | -- | -- | -- |
| 2 | 0.198 | (0.078) | 0.185 | (0.073) | 7.0 | 78.00 | -- | -- | -- |
| 3 | 0.295 | (0.116) | 0.284 | (0.112) | 3.5 | 78.00 | -- | -- | -- |
| 1 | 0.147 | (0.058) | 0.178 | (0.070) | -17.6 | -- | 39.00 | 39.00 | -- |
| 2 | 0.185 | (0.073) | 0.234 | (0.092) | -21.1 | -- | 39.00 | 39.00 | -- |
| 3 | 0.236 | (0.093) | 0.302 | (0.119) | -22.0 | -- | 39.00 | 39.00 | -- |
| 1 | 0.213 | (0.084) | 0.213 | (0.084) | 0.1 | -- | 26.00 | 26.00 | 26.00 |
| 2 | 0.295 | (0.116) | 0.305 | (0.120) | -3.4 | -- | 26.00 | 26.00 | 26.00 |
| 3 | 0.396 | (0.156) | 0.422 | (0.166) | -6.1 | -- | 26.00 | 26.00 | 26.00 |
| 1 | 0.259 | (0.102) | 0.262 | (0.103) | -0.8 | -- | 28.50 | 28.50 | 28.50 |
| 2 | 0.358 | (0.141) | 0.363 | (0.143) | -1.6 | -- | 28.50 | 28.50 | 28.50 |
| 3 | 0.478 | (0.188) | 0.495 | (0.195) | -3.4 | -- | 28.50 | 28.50 | 28.50 |
| 1 | 0.244 | (0.096) | 0.246 | (0.097) | -0.8 | -- | 38.50 | 29.50 | 17.10 |
| 2 | 0.338 | (0.133) | 0.340 | (0.134) | -1.1 | -- | 38.50 | 29.50 | 17.10 |
| 3 | 0.452 | (0.178) | 0.457 | (0.180) | -1.1 | -- | 38.50 | 29.50 | 17.10 |
| 1 | 0.267 | (0.105) | 0.264 | (0.104) | 1.0 | -- | 42.75 | -- | 42.75 |
| 2 | 0.366 | (0.144) | 0.366 | (0.144) | 0.1 | -- | 42.75 | -- | 42.75 |
| 3 | 0.488 | (0.192) | 0.495 | (0.195) | -1.3 | -- | 42.75 | -- | 42.75 |
| 1 | 0.249 | (0.098) | 0.241 | (0.095) | 3.6 | -- | 64.10 | -- | 21.40 |
| 2 | 0.345 | (0.136) | 0.328 | (0.129) | 5.1 | -- | 64.10 | -- | 21.40 |
| 3 | 0.462 | (0.182) | 0.432 | (0.170) | 6.9 | -- | 64.10 | -- | 21.40 |
| 1 | 0.201 | (0.079) | 0.234 | (0.092) | -14.1 | -- | 42.75 | 42.75 | -- |
| 2 | 0.333 | (0.131) | 0.323 | (0.127) | 3.3 | -- | 42.75 | 42.75 | -- |
| 3 | 0.528 | (0.208) | 0.450 | (0.177) | 17.4 | -- | 42.75 | 42.75 | -- |
| 1 | 0.196 | (0.077) | 0.183 | (0.072) | 6.4 | -- | -- | -- | 70.00 |
| 2 | 0.262 | (0.103) | 0.254 | (0.100) | 3.5 | -- | -- | -- | 70.00 |
| 3 | 0.345 | (0.136) | 0.356 | (0.140) | 2.7 | -- | -- | -- | 70.00 |

Number of datum points is 51
Maximum deviations are +17.4% and -22.0%
38 points are within 10%; 49 points are within 20%

$F_a$ = 1.2 STOIC = 30

$F_d$ = 1.3 BPI = 0.4

Powign = 8

Pressures

1- 4.1 MPa (600 psi)
2- 6.9 MPa (1000 psi)
3- 11.0 MPa (1600 psi)

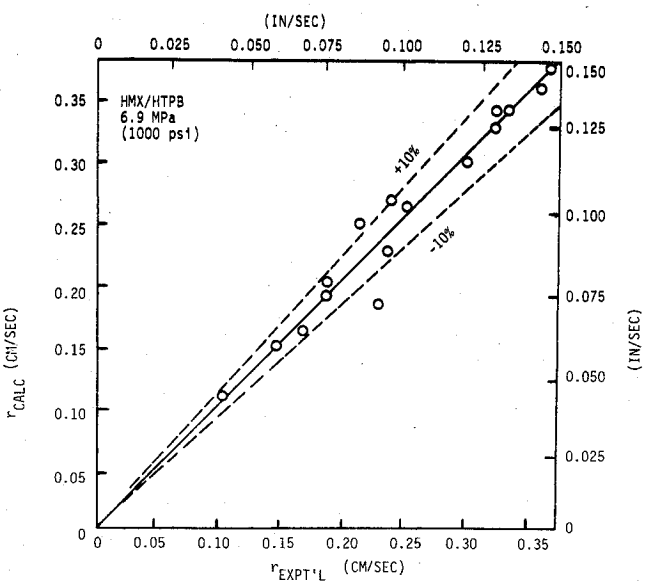


Fig. 6 Comparison of calculated and experimental burning rates.

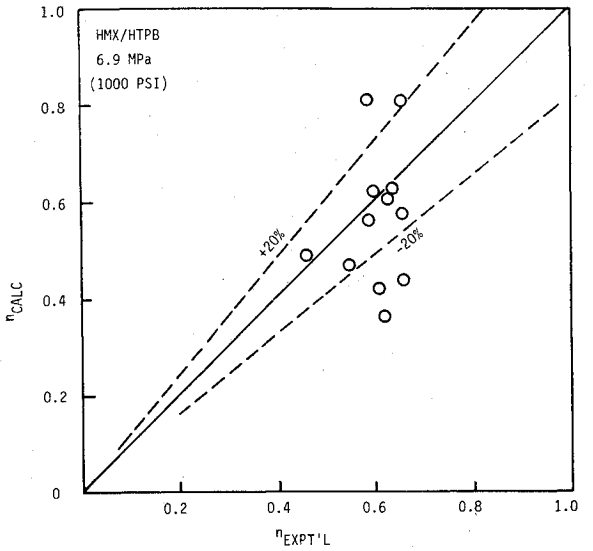


Fig. 7 Comparison of calculated and experimental pressure exponents.

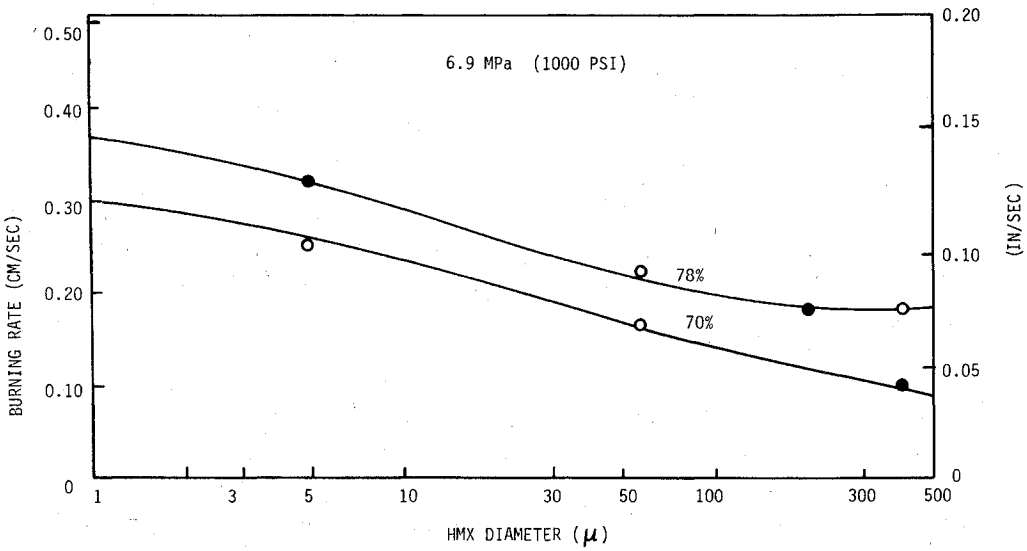


Fig. 8 Predicted burning rate vs partial diameter for monomodal propellants at 70 and 78% solids.

Another trend that is of great interest is the effect of particle size. Calculations are compared to the data for monomodal propellants in Fig. 8. The calculations are similar to the classical S-shaped curve[6] for rate vs the logarithm of particle diameter for AP-composite propellants. For fine particles, the rate is limited by the kinetics of the primary flame. The magnitude of the limiting rate is a function of solids loading due to the interparticle distance $\delta$, which enters into the time-averaging equation [Eq. (8)]. For coarse particles, the rate determination is dominated by the ignition delay time with the interparticle distance causing the observed solids loading effect. The contributions of the four physical mechanisms that control the burn rate are illustrated in Fig. 9. The contribution of each of the four mechanisms has been calculated on a percentage basis and plotted vs the particle diameter. The oxidizer rate is the greatest for fine particles, but the other mechanisms contribute significantly. At 10 $\mu$, the ignition delay time becomes the largest contributor and then increases until it is completely dominant for 100 $\mu$ and larger. For the larger sizes, the oxidizer rate drops to ~10% contribution.

The effect of solids loading on burn rate is shown in Fig. 10. The predicted trends are very interesting, predicting that the various oxidizer sizes from 400 to 5 $\mu$ and distributions from monomodal to trimodal will all converge to a very narrow range of rates at high solids loadings. Experimentally, this trend is difficult to verify since it is impossible to mix the monomodal propellants at solids loadings above 78%, and only one trimodal formulation was made and tested at all three solids loadings. However, a bimodal 200/58 $\mu$ propellant was tested at 78 and 85.5%, and a corresponding 400/58 $\mu$ propellant was tested at 70%. The 400 $\mu$ propellant should be close to the same rate as a 200 $\mu$ propellant; therefore, these three propellants have been included in the figure. Thus, the experimental data appear to confirm the model predictions that the rates do converge at high solids loadings (i.e., 85%).

In addition to direct comparison of the model to experimental results, a series of parametric calculations was made. Calculations were made for bimodal propellants with 70, 78, and 85.5% solids loadings using various combinations of the 5, 58, 200, and 400 $\mu$ particle sizes. Figure 11 shows the results for the combination of 58/5 $\mu$ particle sizes of varying concentrations and coarse/fine ratio. The calculations show the narrow range of rates that might be expected. The rates change in a rather continuous, smooth transition, ranging from the 5 to 58 $\mu$ monomodal propellants at the extremes. Corresponding calculations were made for 200/5, 400/5, and

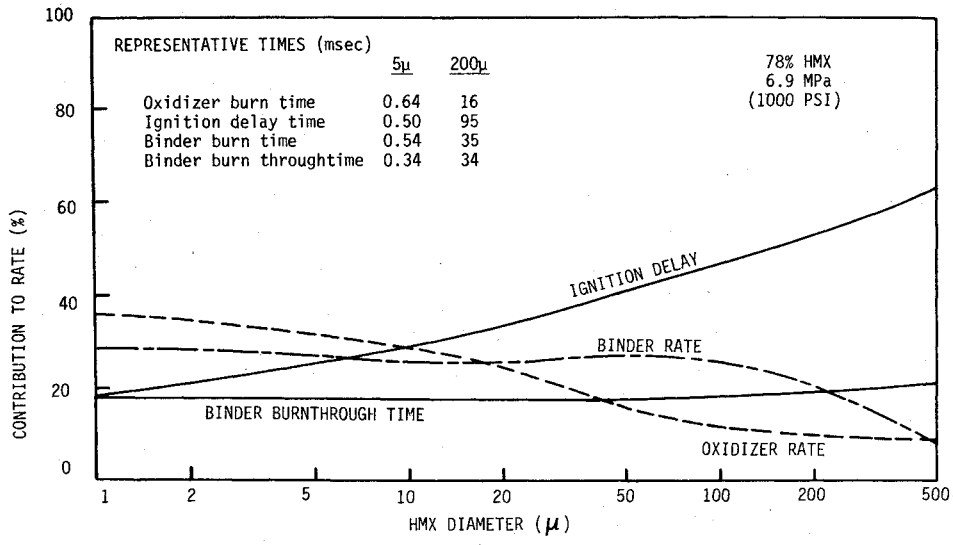


**Fig. 9 Percentage contribution due to combustion mechanisms.**

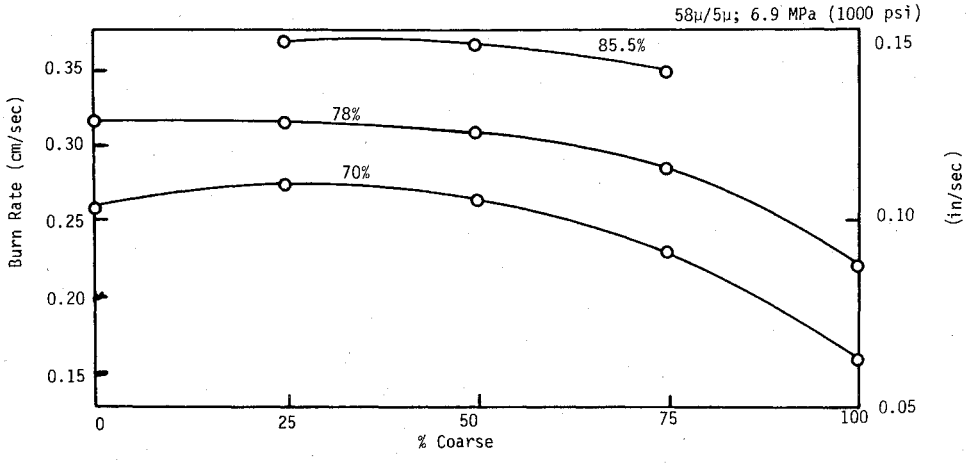


**Fig. 10 Parametric calculations for bimodal HMX/HTPB propellants.**

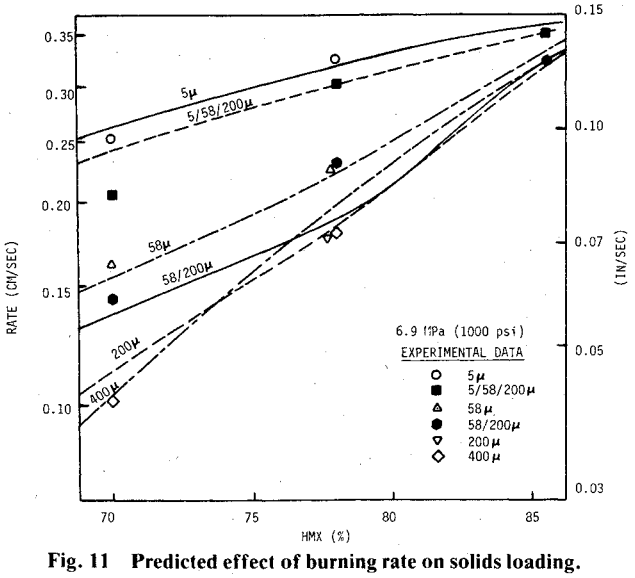


**Fig. 11 Predicted effect of burning rate on solids loading.**

200/58 μ propellants. The nature of the results is very similar, with the exception of the 200/58 μ plot. According to the model, the finest oxidizer size controls the rate, and whenever the fine oxidizer size is 58 μ (or a relatively large size) the model produces some unrealistic fluctuations.

A series of parametric calculations was also made for a trimodal 85.5% propellant containing the 5, 58, and 200 μ HMX. The calculations (Fig. 12) show that propellant burn rate is dominated by the fine oxidizer size over most of the formulation map, with the rate being between 0.35 and 0.37 cm/s (0.14 and 0.15 in./s). The rate drops significantly only for cases where the fine fraction becomes less than 25% of the overall oxidizer loading. These calculations again point out the very narrow range of rates that can be achieved in an HMX propellant.

A detailed examination of the factors within the model that contribute to the rate is enlightening. For cases where the fine fraction is greater than 20%, the fine fraction terms dominate the rate. The oxidizer rate term, the ignition delay term, and the binder burnthrough term are all weighted about equally within the rate equation. This explains why catalysts are not very successful in HMX propellants. The primary flame is the most accessible reaction for a catalyst. If this flame is catalyzed, the net oxidizer rate will increase, but neither the ignition delay time nor the binder burnthrough time will be influenced significantly. Thus, the overall change in the rate would be small. Reducing the ignition delay time would be difficult. One way of modifying the rate would be to change the binder decomposition characteristics significantly. The net conclusion is that catalyzing an HMX propellant should be very difficult. The greatest success should be achieved by modifying the binder decomposition characteristics rather than those of HMX or by using an ignition aid to reduce the ignition delay time.

Data were obtained and have been reported[7,8] varying the binder in HMX propellants. Changes in burning rate were relatively minor for both a polyester and a polyether type binder. Unfortunately, basic thermal pyrolysis data for these binder types are not available for use in the model, and

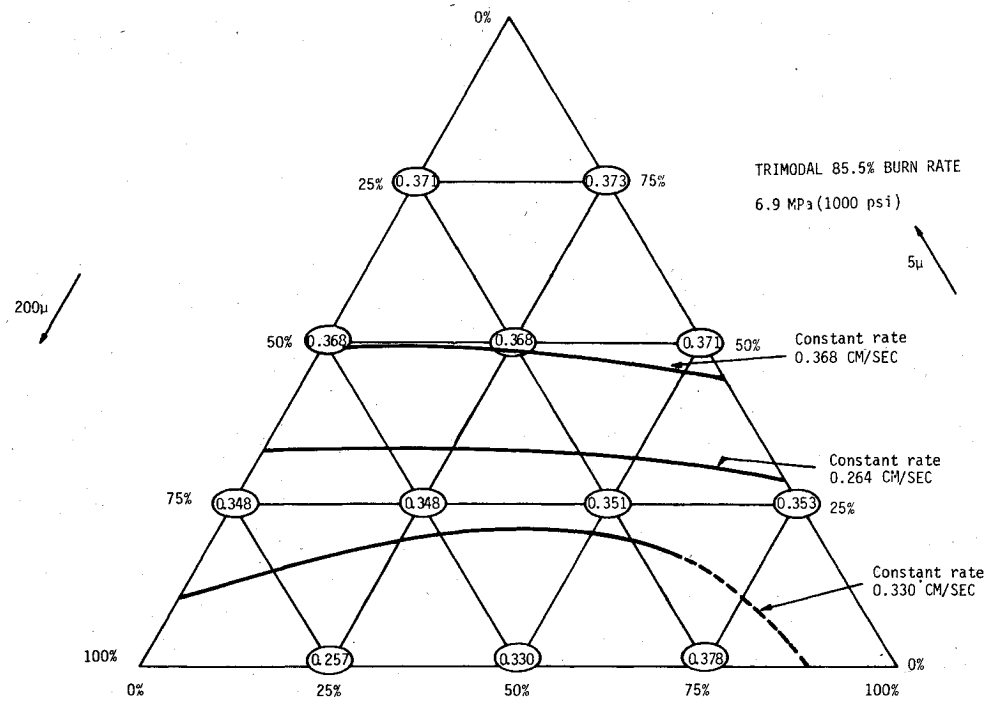


**Fig. 12 Parametric calculations for a trimodal 85.5% HMX/HTPB propellant; circled numbers are burning rates in cm/s.**

therefore, calculations were not made for the corresponding propellants.

### Predicted Temperature Sensitivity

The temperature sensitivity of some of the propellants has been measured in either a strand bomb or in 1-lb test motors. Unfortunately, the data scatter is excessive and the total number of measurements too small to establish quantitative temperature sensitivity values ($\sigma_p$). The data for the HMX/HTPB propellants were carefully analyzed to extract the consistent data. The data [all at 6.9 MPa (1000 psi)] were plotted as log rate vs temperature so that the slope should be the $\sigma_p$. Many of the low-temperature points were higher than the ambient points, giving a negative $\sigma_p$. These data were considered erroneous and were rejected. Additional testing should be performed to verify the validity of this assumption.

The temperature sensitivity data that appear valid have been compared with the model predictions in Fig. 13. Figure 13a shows the data for 298-336 K (77-145°F) plotted vs the ambient rate at 6.9 MPa (1000 psi). Figure 13b shows the 219-298 K (−65-77°F) data. There appears to be a consistent trend in the experimental data in the two temperature regimes. For the high temperature, there is either a slightly increasing trend with increasing rate, or the $\sigma_p$ is constant. At the low temperature, there appears to be a definite decrease in $\sigma_p$ with increasing rate. Within the data scatter, the calculations are in excellent agreement with the data, both in magnitude and the apparent trends. Both the data and the calculations are very significant. The data show the magnitude of the temperature sensitivity for HMX/HTPB propellants, which has not previously been established. The calculations represent the first attempt at calculating the temperature sensitivity of HMX propellants.

In addition to the preceding calculations, parametric calculations were performed for the 85.5% solids propellant. The results are presented in Fig. 14. The particle size distribution was varied for the 5, 58, and 200 $\mu$ particle sizes. A single average value of $\sigma_p$ between 219 and 347 K (−65 and 165°F) was calculated. The results show that the $\sigma_p$ is essentially constant over the range of formulations where the rate is constant. The insensitivity of $\sigma_p$ to formulation was not anticipated.

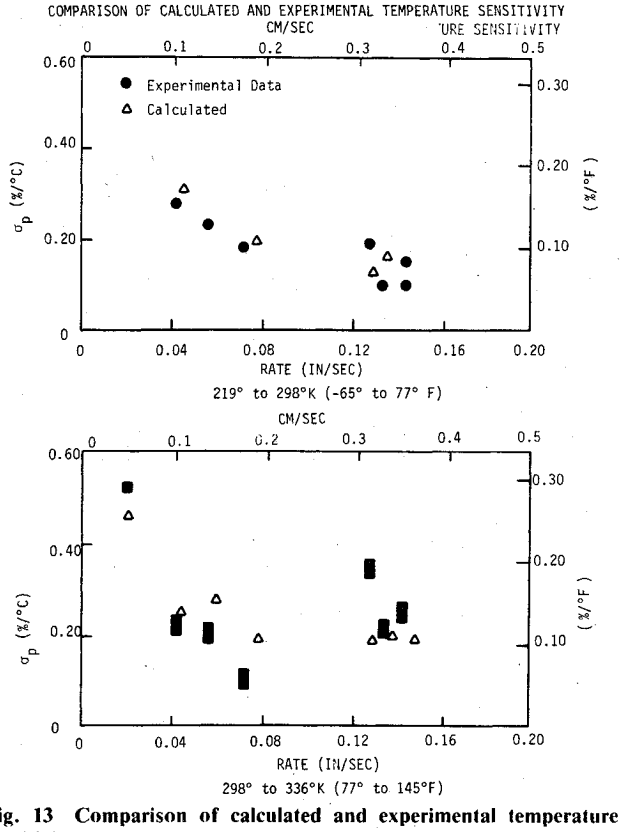


**Fig. 13 Comparison of calculated and experimental temperature sensitivity.**

## Summary and Conclusions

Since the observed combustion behavior of HMX propellants could not be explained by existing models, a new model was developed within the framework of the BDP modeling approach. The newly developed model allows each separate oxidizer type and size fraction to have its own surface temperature, accounting for very wide particle size distributions. A time-averaging approach has been developed assuming that the propellant burns through alternate layers of

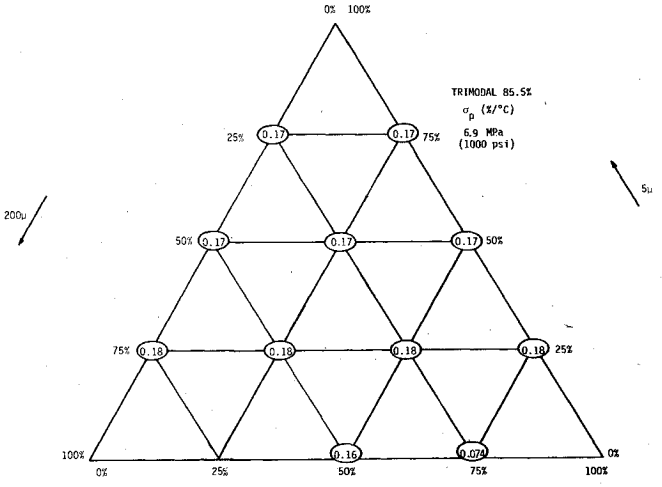


**Fig. 14 Parametric calculations for a trimodal 85.5% propellant; circled numbers are temperature sensitivity in %/°C.**

binder and oxidizer at significantly different rates. This approach leads to the conclusion that all of the binder may not fully react. Therefore, a term representing the fraction of binder that actually reacts has been incorporated into the model to account for time delays due to the unburned binder.

The model has been compared in detail with the experimental results from 17 HMX/HTPB propellants. Formulations varied systematically from 70 to 85.5% solids, 5 to 400 $\mu$ particle size, and monomodal to trimodal oxidizer distributions. Test conditions varied from 2.8 to 12.4 MPa (400 to 1800 psi) and from 250 to 342 K (−10 to 155°F). At ambient temperature, greater than 95% of the predictions are within ±20% of the experimental rates and 75% are within ±10%. The scatter in the temperature sensitivity data is large, but, in general, the predictions are in good agreement with the experimental trends. The model predicts that the rates of HMX/HTPB propellants will converge with increasing solids loadings, and that above ~85% solids there is very little change in rate for varying formulations. The model indicates that changing the rate using conventional catalysis approaches would be difficult, since the rate is more dependent on binder decomposition characteristics than on the oxidizer.

## Acknowledgments

This work was sponsored by AFRPL on Contract F04611-76-C-0019 to Hercules, Inc. The Brigham Young University work was supported by subcontract from Hercules.

## References

[1] Beckstead, M. W., Derr, R. L., and Price, C. F., "A Model of Composite Solid Propellant Combustion Based on Multiple Flames," *AIAA Journal*, Vol. 8, Dec. 1970, pp. 2200-2207.

[2] Beckstead, M. W., Derr, R. L., and Price, C. F., "The Combustion of Solid Monopropellants and Composite Propellants," *Thirteenth Symposium (International) on Combustion*, The Combustion Institute, Pittsburgh, Pa., 1971, pp. 721-730.

[3] Glick, R. L. and Condon, J. A., "Statistical Analysis of Polydisperse Heterogeneous Propellant Combustion: Steady State," *13th JANNAF Combustion Meeting*, Vol. II, CPIA Pub. 281, 1976, pp. 313-345.

[4] Condon, J. A. and Osborn, J. R., "The Effect of Oxidizer Particle Size Distribution on the Steady and Nonsteady Combustion of Composite Propellants," AFRPL-TR-78-17, Purdue Univ., June 1978.

[5] Cohen, N. S. and Price, C. F., "Combustion of Nitramine Propellants," *Journal of Spacecraft and Rockets*, Vol. 12, Oct. 1975, pp. 608-612.

[6] Beckstead, M. W., "Combustion Calculations for Composite Solid Propellants," *13th JANNAF Combustion Meeting*, Vol. II, CPIA 281, Dec. 1976, p. 299.

[7] McCarty, K. P., Isom, K. B., and Jacox, J. L., "Effect of Formulation Variables on HMX Propellant Combustion," *15th JANNAF Combustion Meeting*, Vol. II, CPIA 297, 1979, pp. 11-42.

[8] McCarty, K. P., Beckstead, M. W., Isom, K. B., and Jacox, J. L., "RDX Propellant Combustion," *16th JANNAF Combustion Meeting*, Vol. III, CPIA 308, 1979, pp. 269-288.

[9] Anderson, W. H. et al., "A Model Describing Combustion of Solid Composite Propellants Containing Ammonium Nitrate," *Combustion and Flame*, Vol. 3, Sept. 1959, pp. 301-318.

[10] Beckstead, M. W., presentation at JANNAF HMX Combustion Workshop, Anaheim, Calif., March 1979.

[11] Cohen, N. S., "Report of Workshop on HMX Propellant Combustion Modeling," *16th JANNAF Combustion Meeting*, Vol. III, CPIA 308, 1979, pp. 219-240.

[12] Beckstead, M. W., "A Model for Solid Propellant Combustion," *14th JANNAF Combustion Meeting*, Vol. I, CPIA 292, Dec. 1977, pp. 281-306.

[13] Beckstead, M. W., "A Model for Solid Propellant Combustion," 18th Symposium (Int) on Combustion, The Combustion Institute, Pittsburgh, Pa., 1981, pp. 175-185.

[14] Strahle, W. C., "Some Statistical Considerations in the Burning of Composite Solid Propellants," *AIAA Journal*, Vol. 16, Aug. 1978, pp. 843-847.

[15] Blum, E. N. and Wilhelm, R. H., "A Statistical Geometric Approach to Random-Packed Beds," *AIChE-Industrial Chemical Engineering Symposium*, Ser. 4, London Institute of Chemical Engineers, 1965, pp. 4:21-4:27.

[16] Hermance, C. E., "A Model of Composite Propellant Combustion Including Surface Heterogeneity and Heat Generation," *AIAA Journal*, Vol. 4, Sept. 1966, pp. 1629-1637.

[17] Shannon, L. J. and Peterson, E. E., "Deflagration Characteristics of Ammonium Perchlorate Strands," *AIAA Journal*, Vol. 2, Jan. 1964, pp. 168-169.

[18] Carslaw, H. S. and Jaeger, J. C., *Conduction of Heat in Solids*, 2nd Ed., Oxford University Press, London, 1959.